OPEN ACCESS

Article

Nano Biomed Eng

ISSN 2150-5578 http://nanobe.org

Redox approaches derived Tin (IV) oxide nanoparticles/graphene nanocomposites as the near-infrared absorber for selective human prostate cancer cells destruction

Jin-Sheng Cheng[1] *, Qingqin Liang[2], Haixin Chang[2], Jingying Xu[3], Wenjuan Zhu[1]

[1] School of Pharmacy, Zhejiang Chinese Medical University, Hangzhou 310053, China
[2] Department of Chemistry, Key Lab of Bioorganic Phosphorus Chemistry & Chemical Biology, Tsinghua University, Beijing 100084, China
[3] School of Medicine, Tongji University, Shanghai 200092, China

* Corresponding author: chengjins@gmail.com (J.S. Cheng) Tel/Fax: +86 571 86633171

Abstract

In this paper, Tin (IV) oxide nanoparticles/graphene (SnO_2/GR) nanocomposites were prepared via vacuum thermo treatment of Tin (0) and graphene oxide (GO). A redox reaction would occur readily in this process, in which the novel oxygen donor: GO could act as the oxidizing agent to oxidize Tin (0) to Tin (IV), meanwhile, the graphene precursor: GO would be simultaneously reduced to graphene by Tin (0) readily. The resulted composites were characterized by Fourier transform infrared spectrometry, scanning electron microscopy, and X-ray diffraction spectroscopy ect.. The novel SnO_2/GR nanocomposites could combine both advantages of inorganic metal nanoparticles and graphene for near infrared spectroscopy (NIR) light absorption to generate heat, which fosters SnO_2/GR a special candidate for photothermal ablation therapy (PTA) with NIR. Further investigations show that the SnO_2/GR nanocomposites with NIR features could provide viable option for enhancing the thermal deposition and specificity of hyperthermia treatments for elimination of human prostate cancer (PC3).

Keywords: Graphene, Nanocomposites, Near Infrared, Photothermal Ablation Therapy, Human Prostate Cancer

Citation: J S. Cheng, et al. Redox approaches derived Tin (IV) oxide nanoparticles/graphene nanocomposites as the near-infrared absorber for selective human prostate cancer cells destruction. Nano Biomed. Eng. 2012, 4(2), 76-82. DOI: 10.5101/nbe.v4i2.p76-82.

1. Introduction

Cancer has now become the world's leading cause of death, which claims 7.6 million lives in the world in 2008- more than HIV/AIDS, tuberculosis and malaria combined [1]. Many new strategies for cancer therapies, including photothermal sensitization and PTA with NIR light (light window: 700-1,100 nm), have been explored for treating cancer. The basic principle behind PTA is that heat generated from light can be used to destroy cancer cells. Substantial efforts have been made to develop metal nanostructures with optimal structural and photothermal properties for PTA with NIR. The ideal metal nanostructures should have strong and tunable surface plasmon resonance, low toxicity, be easy to deliver and convenient for bioconjugation with actively targeting specific cancer cells. Recent efforts on PTA with NIR include some inorganic nanomaterials [2-5], such as gold nanoparticles, gold nanorods, silver nanomaterials and carbon nanotube etc., Although these materials show good prospects, some difficulties would also encountered, such as poor bioconjugation for actively targeting specific cancer cells, relative weak surface plasmon resonance absorption and simplex structures. Therefore, new kind of PTA nanomaterial with NIR absorbance is urgently needed.

In the past three years, a novel two-dimensional nanomaterial: graphene has gained increasing interests in different fields [6-7]. This biocompatible carbon-based nanomaterial possesses large surface areas, abundant ripples and few-layered nanosheet structures for drug or imaging agent inclusion. Moreover, graphene can absorb NIR light to generate heat, which making graphene-based materials excellent candidates for all kinds of biomedical applications [8-12]. These novel kind of materials are also expected to show potentials in cancer therapies.

Thanks to the special NIR absorption features of graphene-based materials, the strong absorbance of graphene in the NIR window can penetrate tissues with

minimal attenuation and selectively ablate graphene-targeted cancer cells by localized hyperthermia. The intrinsic physical properties of graphene materials can thus be exploited to afford new types of biological transporters with useful functionalities. Therefore, some researchers had conducted some exploratory work on some kinds of cancer (e.g. Human glioma, U87MG cancer, 4T1 murine breast cancer etc.) therapy methods based on different polymer functionalized graphene or polymer functionalized graphene oxide inclusion in the cell solution and irradiation of the solution by near infrared lasers [13-15]. Another example on NIR application of graphene nanomaterials, Yang and his co-workers applied a PEGylated nano-graphene labeled by an extra NIR fluorescence dye for in vivo fluorescence imaging, and studied the in vivo behaviors of PEGylated nano-graphene oxide (NGO-PEG) in several different xenograft tumor models of mouse, also revealing surprisingly high passive tumor uptake and NIR imaging application of graphene materials [16].

PC3 human prostate cancer cell lines are the classical cell lines of prostatic cancer [17], which were originally derived from advanced androgen independent bone metastasized prostate cancer. Unfortunately, few reports were demonstrated on PC3 human prostate cancer therapy method based on graphene nanomaterials (especially inorganic metal-graphene nanocomposites) inclusion in the cell solution and irradiation of the solution by near infrared lasers. In fact, as we state above, inorganic metal nanoparticles are also very useful NIR materials [9-12]. In this work, by vacuum thermo treatment of inorganic Tin (0) and graphene oxide, the novel SnO_2/GR nanocomposites can be obtained readily. The obtained SnO_2/GR nanocomposites could combine both the advantages of the inorganic metal nanoparticles (typical NIR materials) and graphene (new NIR material) on PTA with NIR.

The purpose of this work is to examine the thermal and biological effects of SnO_2/GR nanocomposites inclusion in monolayer cell cultures during NIR laser therapy. Specifically, this work addressed the effects of SnO_2/GR nanocomposites on heat generation and cell viability. The SnO_2/GR nanocomposites were heated with human prostate cancer PC3 cells to evaluate their thermal properties and significance for use with thermal cancer therapies. Further investigations show that integration of SnO_2/GR into laser hyperthermia treatment could lead to enhanced thermal deposition and specificity to increase PC3 cancer cell injury and minimize injury to healthy tissue.

2. Experimental Details

2.1. Materials and characterization

Graphite powder (99.99995%, 325 mesh) and Tin powder (99.99%, ≤5μm) were purchased from Alfa Aesar. All solvents and other reagents were purchased from Beijing Chemicals Co. Ltd. as analytical-grade products. The SnO_2/GR nanocomposites (1 mg) were poured into 10 mL of PBS solution containing 1% Pluronic F-127 (PL-127) and 2.5% HAc and sonicated for 30 min to obtain a 0.5 mg mL^{-1} homogenous solution. A final solution concentration of 0.1 mg mL^{-1} SnO_2/GR was used for all experiments. Heating of cells with SnO_2/GR was done in PBS with 1% PL-127 and 2.5% HAc. Unheated controls were allowed to seed on slides for 24 hr and then incubated with SnO_2/GR nanocomposites (0.1 mg mL^{-1}) for 24 hours.

The powder X-ray diffraction (XRD) measurements of the samples were recorded on a Bruker D8- Advance X-ray powder diffractometer using Cu Kα radiation (λ=1.5406 Å) with scattering angles (2θ) of 8-60°. JEOL JEM 1200EX and JEOL JEM 2010 transition electronic microscopy were used for transmission electron microscopy (TEM) analysis and high-resolution transmission electron microscopy (HRTEM) analysis at an accelerating voltage of 100 kV, respectively. Samples were prepared by placing one drop of an ethanol suspension of the SnO_2/GR hybrid material onto a copper grid (3 mm, 200 mesh) coated with carbon film. A JSM-7401 scanning electron microscopy (SEM) operated at 20 kV was used to analyze the sample. Raman spectroscopy (Renishaw microprobe RM1000) was recorded at a wavelength of 633 nm (He-Ne laser). Fourier transform infrared (FTIR) spectra were carried out on a Spectrum One (Perkin Elmer) spectrometer from KBr pellets.

2.2. Laser-thermocouple system setup

A continuous wave laser with a beam diameter of 4 mm (Cobolt Rumba™ 1064nm) was used to heat all the test groups in this work. Laser irradiance of 15.3 W/cm^2 (3W, 4 mm beam diameter) and a heating time of 5 min were used for lethal monolayer cell culture experiments. The laser light was coupled to a fiber optic probe that allowed incident light on the center of the culture slide. Two hypodermic thermocouples were placed in the media of the culture chamber at known distances (4 mm from laser center) to measure real-time temperature elevations. A National instruments thermocouple reader (Model SR630) and VI Logger Lite software were used to record temperature data during the experiments. Fig. 1 shows a picture of this laser-thermocouple system setup.

2.3. Spectrophotometer and optical setup

A double-beam Cary 5000 spectrophotometer (Varian, USA) was used to evaluate the optical properties of all the samples in this work. SnO_2/GR sample were made dispersed in phosphate buffered saline (PBS) or deionized water (DI water) for optical assessment. Samples can place in fluorometer or self-masked cuvettes (Starna Cells) and held in the internal DRA integrating sphere cuvette holder. This optical setup would account for scattering effects of the samples.

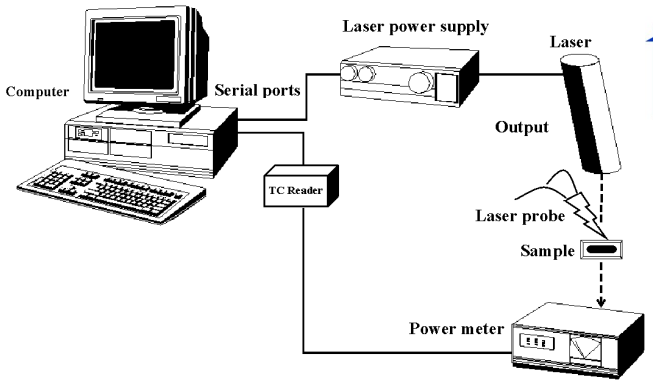

Fig. 1 External beam laser setup for cell heating of this work.

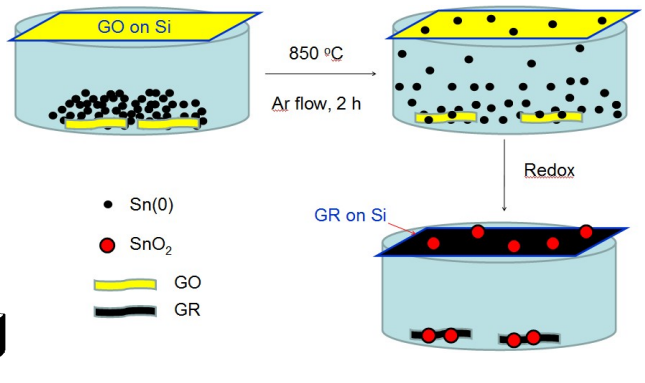

Fig. 2 Illustration of synthesis of the nanocomposite SnO_2/GR.

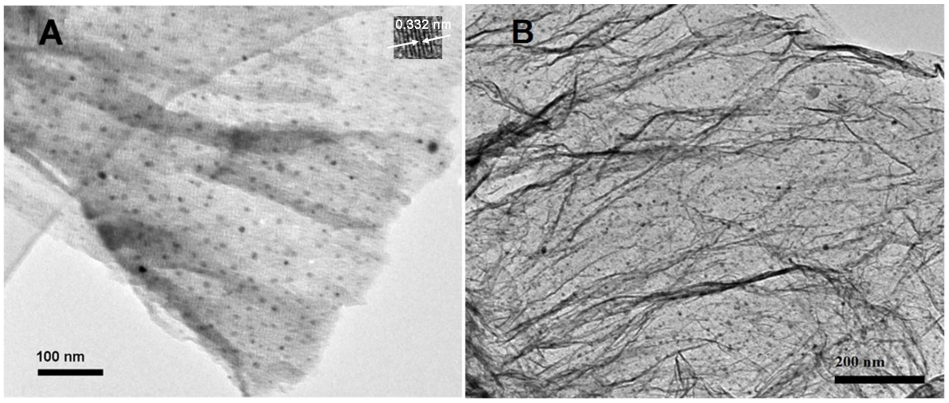

Fig. 3 (A) TEM image of SnO_2/GR, (B) SEM image of SnO_2/GR.

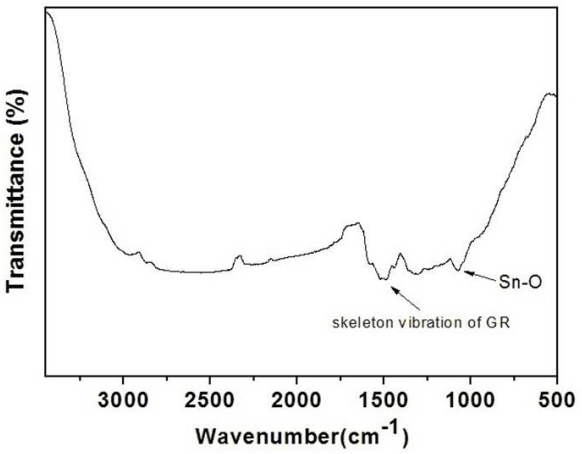

Fig. 4 FTIR spectra of SnO_2/GR.

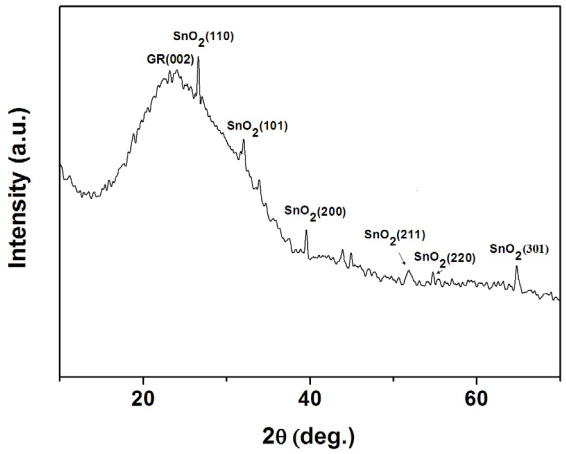

Fig. 5 XRD patterns of SnO_2/GR.

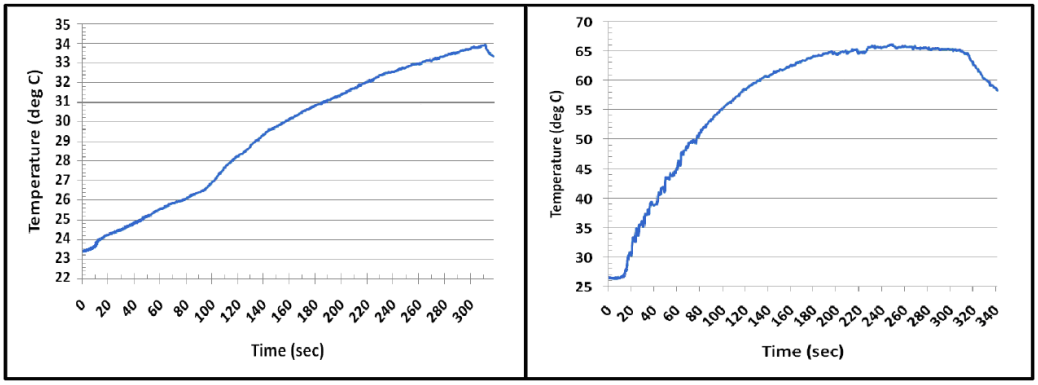

Fig. 6 Temperature graphs for lethal heating (3 W, 5 min, 1064 nm laser) of PBS with 1% PL-127 and 2.5 % HAc (A) without and (B) with 0.1 mg mL^{-1} SnO_2/GR nanocomposites.

2.4. Typical procedures for the synthesis of SnO_2/GR nanocomposites

GO was prepared as previous report [18-20]. In this work, GO powder and Tin (0) (100 mg, 1:2.25) was mixed and ground. The obtained mixture was marked Sn-GO and was put into an alumina boat, a silicon chip with GO coating on the bottom surface was place above the alumina boat, and then the alumina boat together with the samples was placed into a tube furnace and was then heated at 850 ^{o}C for 120 min under argon flow. In such process, Tin (0) with low melting point would evaporate to the surfaces of graphene oxide nanosheets, because the system was controlled at vacuum conditions, thus graphene oxide would be the sole oxygen donor. Graphene oxide would act as the oxidizing agent to oxidize Tin (0) to Tin (IV) readily, meanwhile, the graphene precursor: graphene oxide would also be simultaneously reduced to graphene by Tin (0). After careful collected and vacuum dried, the SnO_2/GR nanocomposites were finally obtained (Fig. 2).

2.5 Cell viability

Trypan blue cell viability studies for unheated SnO_2/GR nanocomposites controls were carried out at 16, 24, and 48 hr post-seeding. Cell viability of lased samples was assessed at 16 hr post-heating using sterile-filtered 0.4 % trypan blue solution (Sigma-Aldrich). For monolayer cell experiments, 0.4 % trypan blue solution was diluted in warmed PBS at a ratio of 1:1. Briefly, culture media was removed and samples were rinsed with warmed PBS twice. Diluted trypan blue solution was placed on samples for 5 min at 25 ^{o}C. Trypan blue was removed and the samples were rinsed twice with PBS. A Leica DMI4000B microscope was used to capture pictures of cell viability.

2.6 Cell culture

A human androgen-independent prostate cancer cell line, PC3 (Sangon Biotech (Shanghai)), was used in these cell experiments. RPMI 1640 media with L-glutamine (J&K) was supplemented with 10 % FBS and 1 % Pen-Strep (Sigma-Aldrich). Cell cultures were kept in a 5 % CO_2 incubator at 37°C in T25 (25 cm^2 area) membrane cap flasks. For cell experiments, cell monolayer cultures were grown on coated 2-chamber glass slides (Fisher Scientific) in a density of 100, 000 cells/chamber (1-2 mL volume) and left to seed for 24 hr before experimentation. During SnO_2/GR heating, culture media was removed and sterile-filtered eagle minimum essential medium (Sigma-Aldrich) was mixed with 0.1 mg mL^{-1} SnO_2/GR and used during heating. Using this media prevented media protein coagulation, which is toxic to cells.

3.Results and discussion

3.1. Characterization SnO_2/GR nanocomposites

Tin (0) possesses quite low melting point (231.89 ^{o}C), which would evaporate to the surfaces of graphene oxide nanosheets, by controlled the system at vacuum conditions; graphene oxide would be the sole oxygen donor. It's interesting that graphene oxide could act as the oxidizing agent to oxidize Tin (0) to Tin (IV) readily, meanwhile, the graphene precursor: graphene oxide would also be simultaneously reduced to graphene by Tin (0). After vacuum dried, the SnO_2/GR nanocomposites were finally afforded. The resulted composites were characterized by FTIR, TEM, SEM and XRD.

The TEM image (Fig. 3A) displays a view of SnO_2/GR nanosheets, clearly illustrating typical flake-like wrinkled shapes of GR. It is observed that SnO_2 nanoparticles are densely decorated on the surface of graphene. These nanoparticles are well separated, appeared spherical in shape, and give a diameter range of 1–3 nm. SEM image shown in Fig. 3B further confirms the effective deposition of SnO_2 nanoparticles on graphene with a narrow particle size distribution. Note that to fully utilize the electrocatalytic property of SnO_2 nanoparticles , it is very important to decorate them on the graphene in a dense and well-dispersed way. It has been reported that the surface groups of carbon such as carboxyl, hydroxyl, and carbonyl groups, which act as anchoring sites for metal ions used for forming the nanoparticles, are crucial for deposition of metal nanoparticles on carbon nanotubes [21]..Therefore, the abundance in chemical functional groups, such as carboxylic, and hydroxyl, in the graphene oxide is also beneficial to anchor Tin (IV) ions, which thus serve an excellent substrate for the formation of SnO_2 nanoparticles on the surface of graphene.

Further evidences supporting the synthesis of SnO_2/GR nanocomposites are supplied by FTIR and XRD. From the FTIR spectra in Fig. 4, a characteristic peak of GR is observed at 1545 cm^{-1} on the curve, which is assigned to the skeletal vibrations of graphene. The spectrum curve of SnO_2/GR also displays one characteristic band Sn-O at about 1100 cm^{-1}, implying the successful loading of SnO_2 nanoparticles on graphene nanosheets [22].

From the XRD patterns in Fig. 5, it is observed that graphene nanosheets give a characteristic peak at 2θ =24.7°, which was in conformity with literature results of GR peak (002) [23-25], confirming that the SnO_2/GR composites still retain the structure of GR. A major characteristic peak of SnO_2 (110) is obtained at 27.2°, suggesting successful oxidization of Tin (0) to Tin (IV). The other four peaks at 32.5°, 37.8°, 51.0° , 54.2°and 63.3° are attributed to (101), (200), (211), (220) and (301) crystalline plane diffraction peaks of SnO_2.

3.2 Temperature and heat generation

An absorption peak is indicative of preferential absorption of that range of wavelengths. In the case of SnO_2/GR, absorption of those preferred wavelengths translates to increased heat generation. To test this theory, a 48-well cell plate was used to assess the temperature of SnO_2/GR samples during 1064 nm laser irradiation.

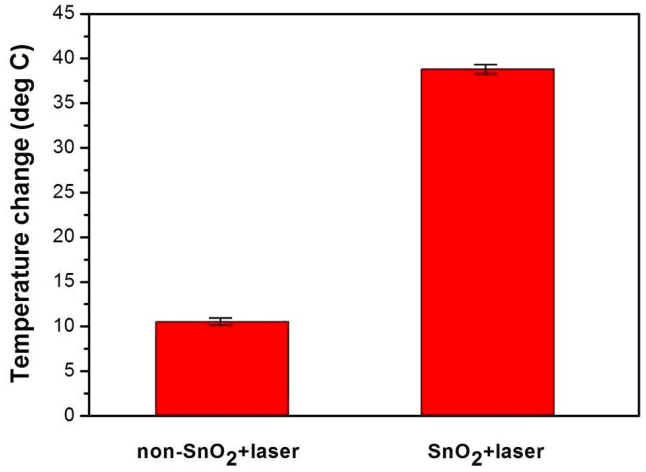

Fig. 7 Temperature elevation without and with SnO_2/GR at lethal laser level (3W, 5min). Concentration of SnO_2/GR was 0.1 mg/mL in PBS with 1 % PL-127 and 2.5 % HAc.

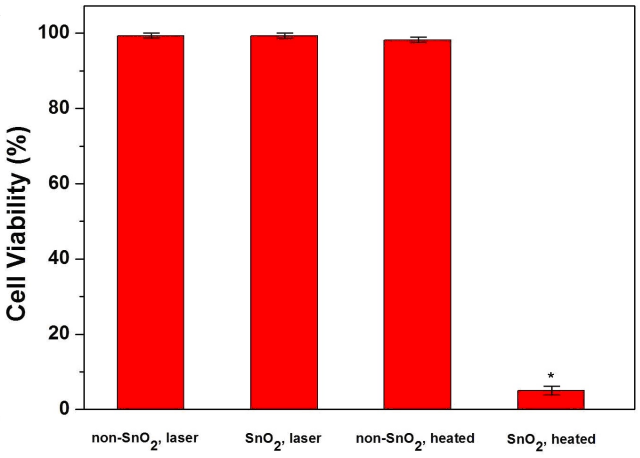

Fig. 8 Cell viability of PC3 cells, note the vital reduction in viable cells with lethal and SnO_2/GR sample. N=3, standard deviations (σ) range: 0.45-3.62 %.

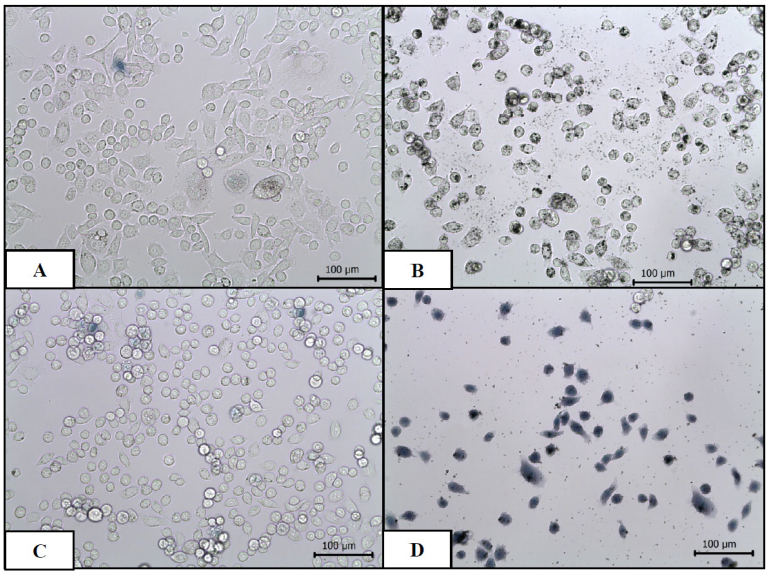

Fig. 9 Trypan Blue staining of PC3 cells: (A) unheated without SnO_2/GR, (B) unheated with SnO_2/GR, (C) lethal heating without SnO_2/GR, and (D) lethal heating with SnO_2/GR. Scale bar is 100 µm.

One thermocouple was placed outside of the laser beam profile. 120 µL of solution of SnO_2/GR nanocomposites was irradiated with a 1064 nm continuous wave laser at 3W power for 5 min (lethal setting). Maximum temperatures for non-SnO_2/GR and SnO_2/GR samples were 33.95 °C and 65.46 °C, respectively, with a standard deviation range between 0.70-1.15 °C. Temperature profiles are shown for non-SnO_2/GR and 0.1mg mL^{-1} SnO_2/GR samples in Fig. 6.

Temperatures rose within the non-SnO_2/GR and 0.1 mg/mL SnO_2/GR samples by 10.52 °C and 38.81°C, respectively. Fig. 7 shows this significant different in temperature elevation. The SnO_2/GR samples showed higher maximum temperatures and larger temperature elevations compared to their non-SnO_2/GR counterparts, which displayed the ability of SnO_2/GR to couple to NIR light to generate heat.

3.3 Cell viability

Cell viability remained high and comparable within the control groups. Upon laser applications, the non-SnO_2/GR samples possessed a similar cell viability compared to controls. The only significant difference was seen in the lethal heating of samples with SnO_2/GR inclusion. Fig. 8 demonstrates trypan blue staining of PC3 control and lethal heated cells. Mean cell viability for unheated non-SnO_2/GR samples was 99.25 %, for unheated SnO_2/GR samples 99.37 %, for lethally heated non-SnO_2/GR samples was 98.24 %, and for lethally heated SnO_2/GR samples 5.03 % (see Fig. 8). The standard deviations ranged from 0.45-3.62 %.

Fig. 9 shows trypan blue staining of PC3 control and lethal heated cells. As we can see from Fig. 9A and Fig. 9B, for unheated non-SnO_2/GR samples (control) and

unheated SnO_2/GR samples, similar high cell viability results were observed, no obvious apoptosis effects of some PC3 cell were observed, indicates that a NIR irradiation is necessary. Meanwhile, lethally heated non-SnO_2/GR samples show 98.24 % cell viability (Fig. 9C), which present only slightly decrease comparing with control samples (Fig. 9A), indicating that without SnO2/GR, temperature elevations was not high enough for thermal injury and PC3 cell death. By lethal combination with NIR laser, significant temperature elevations were observed in the lethal heated SnO_2/GR samples, these elevations were above the threshold necessary for irreversible thermal injury and cell death. Therefore, cell viability decreased sharply (Fig. 9D). The dramatic difference in cell viability in the heated SnO_2/GR samples demonstrated the potential of SnO2/GR as a thermal enhancer to effectively kill cancer cells. This feature could be used to target cancer cells or other cells of interest by attachment of specific antibodies.

4. Conclusion

The SnO_2/GR nanocomposites hold large surface areas, rich ripples and few-layered graphene structures for drug or imaging agent inclusion, especially NIR light absorption to generate heat, which foster SnO_2/GR nanocomposites excellent candidates for PTA with NIR. In this work, an significantly temperature elevations can be observed in a range of 0.025 mg mL^{-1} and 0.3 mg mL^{-1} SnO_2/GR solutions upon 1064 nm laser irradiation of 1-5W. Cell viability remained high in all the groups of the study except the lethal laser group with SnO_2/GR (cell viability=5.03 %), which reveals that SnO_2/GR nanocomposites were not inherently toxic to the cells. The lethal combination of SnO_2/GR and NIR laser light shows these SnO_2/GR composites as viable options for enhancing the thermal deposition and specificity of hyperthermia treatments for elimination of human prostate cancer. Integration of SnO_2/GR into laser hyperthermia treatment could lead to enhanced thermal deposition and specificity to increase PC3 cancer cell injury and minimize injury to healthy tissue. Enhancing thermal therapies and optimizing those combined therapies could decrease recovery times and reduce the risk of tumor recurrence.

Acknowledgements

This work was financially supported by the Guangxi Zhuang Autonomous Region Science Foundation of China (No. 2011GXNSFA 018149).

References

01. Ferlay J, Shin HR, Bray F, Forman D, Mathers C. GLOBOCAN 2008, Cancer Incidence and Mortality Worldwide in 2008. 2008;International Agency for Research on Cancer.
02. Hirsch LR, Stafford RJ, Bankson JA, Sershen SR, Rivera B, Rice RE, Hazle JD, Halas NJ, West JL. Nanoshell-mediated near-infrared thermal therapy of tumors under magnetic resonance guidance. *Proc. Nat. Acad. Sci.* 2003;100:13549-13554.http://dx.doi.org/10.1073/pnas.2232479100
03. Everts M, Saini V, Leddon JL, Kok RJ, Stoff-Khalili M, Preuss MA, Millican CL, Perkins G, Brown JM, Bagaria H, Nikles DE, Johnson DT, Zharov VP, Curiel DT. Covalently linked Au nanoparticles to a viral vector: potential for combined photothermal and gene cancer therapy. *Nano. Lett.* 2006;6:587-591.http://dx.doi.org/10.1021/nl0500555
04. Huang X, El-Sayed IH, Wei Q, El-Sayed MA. Cancer Cell Imaging and Photothermal Therapy in the Near-Infrared Region by Using Gold Nanorods. *J. Am. Chem. Soc.* 2006;128:2115-2120. http://dx.doi.org/10.1021/ja057254a
05. Kam NWS, O'Connell M, Wisdom JA, Dai HJ. Carbon nanotubes as multifunctional biological transporters and near-infrared agents for selective cancer cell destruction. *Proc. Nat. Acad. Sci.* 2005;102(33):11600-11605.http://dx.doi.org/10.1073/pnas.0502680102
06. Feng LZ, Liu Z. Graphene in biomedicine: opportunities and challenges. Nanomed. 2011;6(2):317-324.http://dx.doi.org/10.2217/nnm.10.158
07. Mohanty N, Berry V. Graphene-based Single-Bacterium Resolution Biodevice and DNA-Transistor-Interfacing Graphene-Derivatives with Nano and Micro Scale Biocomponents. *Nano. Lett.* 2008;8:4469-4476.http://dx.doi.org/10.1021/nl802412n
08. Zhang LM, Xia JG, Zhao QH, Liu LW, Zhang ZJ. Functional Graphene Oxide as a Nanocarrier for Controlled Loading and Targeted Delivery of Mixed Anticancer Drugs. *Small* 2010;6:537-544.http://dx.doi.org/10.1002/smll.200901680
09. Yang XY, Zhang XY, Liu ZF, Ma YF, Huang Y, Chen Y. High-Efficiency Loading and Controlled Release of Doxorubicin Hydrochloride on Graphene Oxide *J. Phys. Chem. C* 2008; 12:17554-17558.http://dx.doi.org/10.1021/jp806751k
10. Liu Z, Robinson JT, Sun XM, Dai HJ. PEGylated Nanographene Oxide for Delivery of Water-Insoluble Cancer Drugs. *J. Am. Chem. Soc.* 2008;130:10876-10877.http://dx.doi.org/10.1021/ja803688x
11. Sun XM, Liu Z, Welsher K, Robinson JK, Goodwin A, Zaric S, Dai HJ. Nano-graphene oxide for cellular imaging and drug delivery. *Nano. Res.* 2008;1:203-212.http://dx.doi.org/10.1007/s12274-008-8021-8
12. Nayak TR, Andersen H, Makam VS, Khaw C, Bae S, Xu XF, Ee PL, Ahn JH, Hong BH, Pastorin G, Özyilmaz B. Graphene for Controlled and Accelerated Osteogenic Differentiation of Human Mesenchymal Stem Cells. *ACS Nano*. 2011;5:4670-4678. http://dx.doi.org/10.1021/nn200500h
13. Markovic ZM, Harhaji-Trajkovic LM, Todorovic-Markovic BM, Kepić DP, Arsikin KM, Jovanović SP, Pantovicc AC, Dramićanina MD, Trajkovic VS. In vitro comparison of the photothermal anticancer activity of graphene nanoparticles and carbon nanotubes. *Biomaterials* 2011;32(4):1121-1129.http://dx.doi.org/10.1016/j.biomaterials.2010.10.030
14. Robinson JT, Tabakman SM, Liang YY, Wang HL, Casalongue HS, Vinh D, Dai HJ. Ultrasmall Reduced Graphene Oxide with High Near-Infrared Absorbance for Photothermal Therapy. *J. Am. Chem. Soc.* 2011;33 (17):6825-6831.http://dx.doi.org/10.1021/ja2010175
15. Yang K, Wan J, Zhang S, Tian B, Zhang Y, Liu Z. The influence of surface chemistry and size of nanoscale graphene oxide on photothermal therapy of cancer using ultra-low laser power. *Biomaterials* 2012:33(7):2206-2214.http://dx.doi.org/10.1016/j.biomaterials.2011.11.064
16. Yang K, Zhang S, Zhang G, Sun X, Lee ST, Liu Z. Graphene in Mice: Ultrahigh In Vivo Tumor Uptake and Efficient Photothermal Therapy. *Nano Lett.* 2010;10(9):3318-3323.http://dx.doi.org/10.1021/nl100996u
17. Alimirah F, Chen J, Basrawala Z, Xin H, Choubey D. DU-145 and PC-3 human prostate cancer cell lines express androgen receptor: implications for the androgen receptor functions and regulation. *FEBS Lett.* 2006;580(9):2294-2300.http://dx.doi.org/10.1016/j.febslet.2006.03.041
18. Hummers WS, Offeman RE. Preparation of graphitic oxide. *J. Am. Chem. Soc.* 1958; 80:1339-1139.http://dx.doi.org/10.1021/ja01539a017
19. Cheng JS, Tang LH, Xu JY. An Economical, Green Pathway to Biaryls: Palladium Nanoparticles Catalyzed Ullmann Reaction in Ionic Liquid/Supercritical Carbon Dioxide System. *Adv. Syn. Catal.* 2010;52:3275-3286.http://dx.doi.org/10.1002/adsc.201000475

20. Geim AK. Graphene: Status and Prospects. *Science.*2009;324(5934): 1530-1534.http://dx.doi.org/10.1126/science.1158877
21. Ismaili H, Lagugne-Labarthet F, Workentin MS. Covalently Assembled Gold Nanoparticle-Carbon Nanotube Hybrids via a Photoinitiated Carbene Addition Reaction. *Chem. Mater.* 2011;23(6):1519-1525.http://dx.doi.org/10.1021/cm103284g
22. Mi FL. Synthesis and characterization of a novel chitosan-gelatin bioconjugate with fluorescence emission. Biomacromolecules 2005;6:975-987.http://dx.doi.org/10.1021/bm049335p
23. Cheng JS, Tang LH, Li JH. Palladium Nanoparticles-Decorated Graphene Nanosheets as Highly Regioselective Catalyst for Cyclotrimerization Reaction. J. Nanosci. Nanotech. 2011;11:5159-5168.http://dx.doi.org/10.1166/jnn.2011.4173
24. Cheng JS, Du J. In-Situ Synthesis of Germanium-Graphene Nanocomposites and their Application as Anode Material for Lithium Ion Batteries. *CrystEngComm*. 2012;14 (2):397-400. http://dx.doi.org/10.1039/c1ce06251d
25. Cheng JS, Du J, Zhu WJ. Facile Synthesis of Three-Dimensional Chitosan- Graphene Mesostructures for Reactive Black 5 Removal. Carbohydr. *Polym*. 2012;88(1):61-67.http://dx.doi.org/10.1016/j.carbpol.2011.11.065